Self-Protection Characteristic Comparison between No-Insulation, Metal-as-Insulation, and Surface-Shunted-Metal-as-Insulation REBCO coils

Junseong Kim, Dongkeun Park, Fangliang Dong, Andrew Lanzrath, Wooseung Lee, Juan Bascuñán, and Yukikazu Iwasa

***Abstract*— The metal tape co-winding or a metal-as-insulation (MI) winding method is an excellent way to improve the mechanical properties and reduce the average current density, thereby decreasing the stress in high-field REBCO magnet without completely losing the benefits of the no-insulation (NI) winding method. However, the MI winding increases the resistance between turns, which is known as characteristic resistance. The increased characteristic resistance can reduce the bypass current during abnormal transition situation, such as quench, which may not be desirable from a magnet protection point of view. To take advantage of both the MI and NI winding, one possible solution to reduce characteristic resistance of the MI winding coils is to add a shunt on top of the winding surface of the coil. We call this method surface-shunted-metal-as-insulation (SSMI). In this presentation, we compare the characteristic resistances and their correlated self-protecting characteristics between NI, MI, and SSMI. We present the test results of single pancake coils which wound using different winding methods (NI, MI, and SSMI) with same winding pressure of 20 N. In particular, we investigated how the SSMI method affects the characteristic resistance.**

***Index Terms*—Metal-as-insulation, No-insulation, REBCO magnet, Self-protection, Surface-shunted.**

I. Introduction

NUMEROUS experiments have validated the impressive self-protection characteristic of the no-insulation (NI) high-temperature superconducting (HTS) coils. The key idea of the NI winding technique is to completely eliminate turn-to-turn insulation during winding process [1] . When abnormal situations such as a local hot spot in an NI HTS coil or external power supply shutdowns occur, the current that was originally flowing in the azimuthal direction through superconducting layer is automatically bypassed to the resistive turn-to-turn path [2]–[4]. This bypass allows the coil to flow current beyond the critical current (I_C) and prevents the coil from overheating and consequently from burning, which is called self-protection. Conventional insulated HTS magnet cannot operate at high current density due to protection issue; as the maximum allowable matrix current density determines the operating current [5]. However, the self-protection characteristic of the NI HTS (specifically, REBCO) magnet enables it to operate at much higher overall current density (even ≥1500 A/mm^2) [6], making it more compact than conventional insulated magnets. As the recent I_C performance of REBCO conductors at low temperature under high field has considerably improved [7]–[9], it is now possible to design high-field magnets with higher operating current densities, which in turn require less conductor length, thereby reducing costs.

As the current density increases, NI REBCO magnets also face mechanical stress issues. Although they are more robust than conventional insulated magnets, which contain more soft materials such as insulation and copper, the hoop stress increases with current density. To design a high-field magnet with a medium-to-large bore using a high-I_C-performance REBCO conductor, increasing the conductor thickness may be necessary. Metal-as-insulation (MI) co-winding with high-strength metal tape, such as stainless steel (SS) or Hastelloy, is preferable to using thicker-copper-plated REBCO tape due to higher mechanical strength [10], [11]. However, MI coils have higher turn-to-turn resistance, or characteristic resistance, which decreases their self-protective capacity against overheating, overcurrent, and sudden discharging compared to NI coils. In some harsh operating conditions initiated by turn-to-turn heating after the external power supply is shut off, even NI coils can quench, which is a sudden loss of superconductivity [12], [13].

To prevent quench, we suggested applying an external shunt resistor across the NI coil, which enhances its self-protecting capability [14]-[16]. However, the MI coil is even more vulnerable to quench in this situation, as it is a trade-off method between self-protecting ability and mechanical stress. To address this issue, we propose a surface-shunted-metal-as-insulation (SSMI) winding method that secures both mechanical strength and self-protecting capability, while maintaining a decent overall current density. We built and tested three small-scale single-pancake REBCO test coils with NI, MI, and SSMI winding methods to demonstrate and compare their self-protecting performance.

Research reported in this publication was supported by the National Institute of General Medical Sciences of the National Institutes of Health under award number R01GM137138. *(Corresponding author: Dongkeun Park.)*

J. Kim, D. Park, F. Dong, A. Lanzrath, J. Bascuñán, and Y. Iwasa are with the Plasma Science and Fusion Center (PSFC), Massachusetts Institute of Technology (MIT), Cambridge, MA 02139, USA. (e-mail: dk_park@mit.edu).

W. Lee was with the PSFC, MIT, Cambridge, MA 02139, USA. He is now with Gwangju Center, Korea Basic Science Institute, Buk-gu, Gwangju, 611856, South Korea. (e-mail: wlee2022@kbsi.re.kr).

Template version 8.0d, 22 August 2017. IEEE will put copyright information in this area
See http://www.ieee.org/publications_standards/publications/rights/index.html for more information.

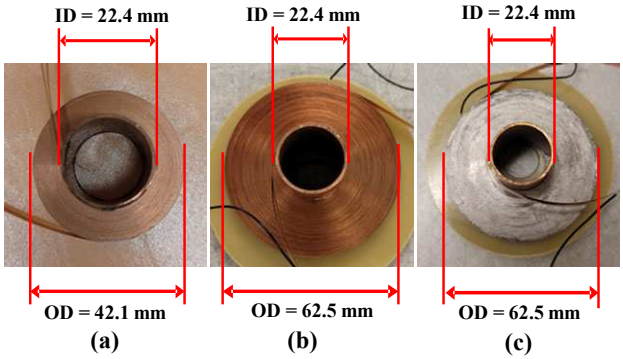

Fig. 1. Pictures of three types of NI REBCO test coils: (a) conventional NI; (b) MI; and (c) SSMI coils.

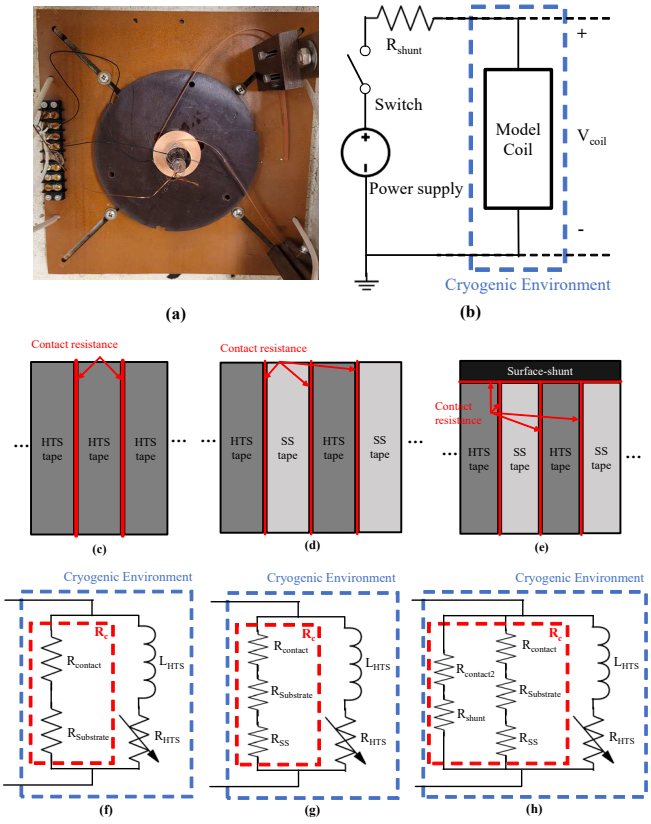

Fig. 2. (a) Picture of model coil and measurement array, (b) schematic diagram of the test circuit; Schematic cross-section view of (a) NI, (b) MI, and (c) SSMI coil; Simple equilibrium circuit model with characteristic resistances of (a) NI, (b) MI, and (c) SSMI coil.

II. Three Types of Test Coils: NI, MI, and SSMI

We selected the REBCO tapes produced by SuperPower with a width of 6 mm and a thickness of 76 µm (with approximately 10 µm copper on each side) left over from our previous experiment [17] to construct three single pancake test coils. The NI coil was wound with 130 turns using a winding tension of 20 N on a copper bobbin with an inner diameter of 22.4 mm, as shown in Fig. 1a, with the cross-section and circuit model of the NI coil illustrated in Fig. 2c and 2f. In Fig. 2c, the red lines represent the contact resistance between each turn of the NI coil. This copper bobbin also serves as a current terminal for the single pancake coil. The OD of the NI coil is 42.1 mm. For the MI coil, we utilized full-hard SS 304 tape for co-winding, with the same 20 N winding tension applied to both the REBCO and SS tapes. We have made MI coils in the same turn as NI coil. Fig. 1b demonstrates that the MI coil's OD is larger than the NI coil's OD due to co-winding, resulting in a larger cross-sectional area for the same ampere-turns. The cross-section and circuit model of the MI coil illustrated in Fig. 2d and 2g. As we made the SSMI coil using the MI coil in the Fig 1c, the coil parameters of the SSMI coil are essentially the same as those of the MI coil. Table I displays the parameters and computed inductance of the three coils, with the cross-section and circuit model of the SSMI coil illustrated in Fig. 2e and 2h.

TABLE I
Specification of REBCO Test Coils

Parameter	NI coil	MI (SSMI) coil
REBCO width; thickness	6 mm; 76 µm	
Conductor Ic @ 77K, self-field	173 A	
SS tape width; thickness	N/A	6 mm; 78 µm
Winding ID; OD [mm]	22.4; 42.1	22.4; 62.5
Number of turns	130	
Total length [m]	13.2	17.4
Computed inductance [µH]	560	650

TABLE II
Properties of Solders

Solder	Melting Point [ºC]	ρ (300K) [10^{-7}Ω·m]	ρ (77K) [10^{-7}Ω·m]	T_C [K]	B_{C2} [T]
Cerrolow 136	58	9.4	8.1	6.4	3.3
$In_{52}Sn_{48}$	118	2.6	1.3	6.4	0.34
$Pb_{38}Sn_{62}$	183	1.5	0.48	7.3	0.3

The SSMI coil was created by soldering onto the top surface of the previously made and tested MI coil, as shown in Fig. 2e. In Fig. 2e, the red lines represent the contact resistance between each turn and surface shunt with HTS tapes. The impact of delamination of solder on the HTS tape would be very small because the solder is just applied to the top surface of the coil. While there have been some preliminary studies on soldered-metal-insulation coils [18]-[20], these approaches used pre-tinned tapes, and therefore the thickness of the solder layers between turns cannot be neglected, which does not target maintaining the mechanical strength of the MI coil. After testing was completed, the MI coil was warmed and dried before being placed on a heat plate and heated to 80 °C for soldering using Cerrolow 136 ($Bi_{49}Pb_{18}In_{21}Sn_{12}$) [21]. To create a surface-shunt after the coil winding was completed, an $In_{52}Sn_{48}$ solder (melting point: 118°C) was used to affix the end turns of the coil, while the lower-temperature solder (or fusible alloy) Cerrolow 136 (melting point: 58°C) was used as solder to avoid melting and failing the coil winding. Properties of the selected solders are listed in Table II. It should be noted

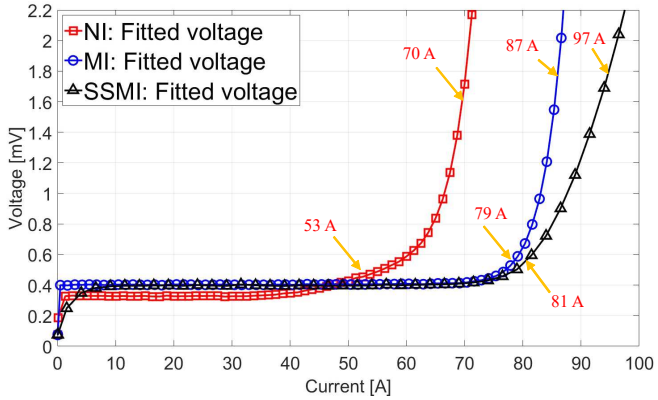

Fig. 3. Experimental results graph for Ic test

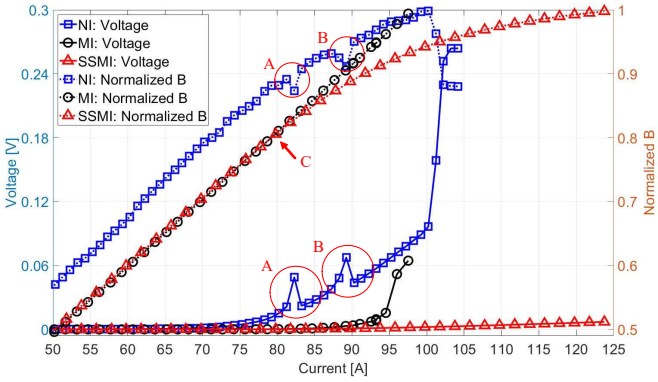

Fig. 4. Experimental results graph for over current test.

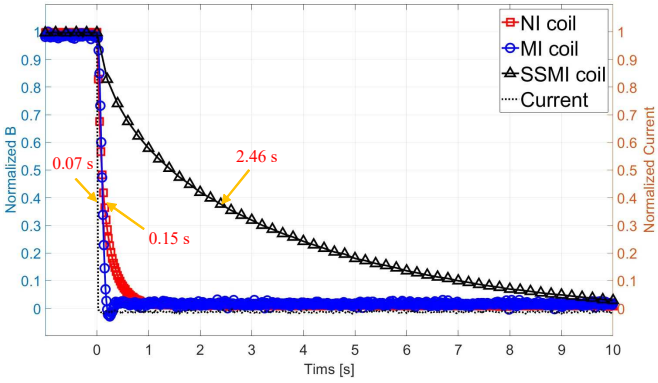

Fig. 5. Experimental results graph for discharging test

that Cerrolow 136 is superconducting at < 3 T and below 6.4 K and is therefore not a good option for a magnet operating under 6.4K. If this solder used as a shunt and tested at under 6.4 K, the coil may not be able to ramp up due to the superconducting shunt.

We constructed a test environment such as the circuit shown in Fig. 2a and 2b. Characteristic resistance, which includes all resistance such as surface shunt resistance, SS tape resistance, is placed in parallel with the resistance and inductance of the superconducting coil, and the current bypassed was denoted as I_r. The NI and SSMI coils were subjected to a sudden discharge test using a switch, while for the MI coil test, the power supply was simply turned off without using a switch. The three coils were tested at 77 K using a liquid nitrogen bath. A Toshiba THS118 (GaAs type) hall sensor was placed at the center of the coils to measure the center field. The power supply current and voltage across the coil end turns were also measured. To compare the self-protecting characteristics, we obtained the characteristic resistance of the NI, MI, and SSMI by conducting charging and discharging experiments. Additionally, we performed over-I_C-current charging tests to compare the thermal runaway characteristic under liquid-nitrogen cooling conditions.

TABLE III
SPECIFICATION OF COILS

Parameter	NI coil	MI coil	SSMI coil
Inductance [μH]	509.4	651.3	643.5
Ic @ 77K [A]	53	79	81
Time constant, τ [s]	0.15	0.07	2.46
Characteristic resistance, R_c[mΩ]	3.396	9.304	0.262 0.284 ($R_{c,shunt}$)
Surface contact resistivity, ρ_{ct}[μΩ·cm^2]	153.5	262.9	7.4 8 ($\rho_{ct,shunt}$)

III. RESULTS AND DISCUSSION

Initially, the I_C of each coil was measured at 77K using a ramp rate 0.5 A/s, and the results are shown in Fig. 3. We used the 0.1 μV/cm criterion for higher sensitivity, resulting in I_C values 53 A, 79 A, and 81 A for the NI, MI, and SSMI coils, respectively. The 1 μV/cm criterion yielded I_C values of 70 A, 87 A, and 97 A for the same coils. An overcurrent test was also conducted, and the results are shown in Fig. 4. While bypass current through contact resistance needs to be considered to obtain more accurate I_C value [22], Fig. 4 indicate that there is no bypass current under the critical current of each coil. However, over the critical current, the magnetic field will saturate due to bypass current. Therefore, the 0.1 μV/cm criterion is suitable for this experiment. The NI coil has the lowest I_C because it has the highest current density and experience the highest penetrated magnetic field into the conductor compared to the other coils. The difference in I_C between the MI and SSMI coils, which are essentially the same coil except for the surface-shunt, can be attributed to the difference in contact resistance, affecting the resistive voltage rise during the superconducting to normal transition. The surface-shunt in the SSMI coil leads to a reduced voltage during the transition state, indicating slightly higher I_C compared to that of the MI coil.

The characteristic resistance and surface contact resistivity widely used as an index to compare the self-protecting performance of NI coils. To determine these values, it is necessary to obtain the time constant of the coil. We conducted a discharging test at an operating current of 20 A, which is sufficiently lower than I_C of each coil. In this condition, the R_{HTS} is negligible and can be disregarded. The NI and SSMI coils

were discharged using the switch shown in Fig. 2b, whereas the power supply was turned off for the MI coil test. The experimental results are graphically presented in Fig. 5, and the decay time constant of each coil is summarized in Table III. By substituting the time constant into (1), the characteristic resistance, R_c, can be obtained.

$$R_c = \frac{L_{coil}}{\tau} \tag{1}$$

Where L_{coil} is the inductance of the coil. The inductance was obtained from the $L_{coil} \cdot dI/dt$ in the current charging sequence and these values are well consistent with the computation in Table I. For removing the influence of the coil shape, the surface contact resistivity, ρ_{ct}, was calculated using (2) because the shape of the NI coil and the MI/SSMI coil are different.

$$R_c = \sum_{i=1}^{N-1} \frac{\rho_{ct}}{2\pi r_i w} \tag{2}$$

Where r_i is the winding radius of the i-th HTS tape, and w is the HTS width. ρ_{ct} was obtained by summing the reciprocal of the length of each turn and then multiplying the obtained R_c. The obtained values are summarized in Table III. The characteristic resistance circuit model of the MI and SSMI coil is illustrated in Fig. 2g, 2h, respectively and can be expressed as a parallel connection of the shunt component, $R_{c,shunt}$, and the $R_{c,MI}$ of the MI coil. To determine the component resulting from the added shunt in the SSMI coil, the parallel circuit equation of resistance, $1/R_{c,MI} + 1/R_{c,shunt} = 1/R_{c,SSMI}$, can be used. The value obtained is 0.284 mΩ, and $\rho_{ct,shunt}$ can be calculated as 8 $\mu\Omega \cdot cm^2$. By applying this separation and calculation method, appropriate selection of solder, application thickness, and width for the system can be determined.

We conducted over current test and the results of the test are presented in the Fig. 4, which shows both coil voltages and center fields versus current up to maximum 125 A. Since the NI coil has a higher center field than the other two coils and the hall sensor position were inaccurate causing a field difference, the field was normalized to enable a more intuitive comparison. All three coils were charged normally with some delays up to their I_C. When the current passed the I_C of the NI coil, the voltage started increasing slowly up to ~67 A, and then increased more quickly after passing 67 A. At around 82 A and 89 A (Point A and B, respectively, in Fig. 4), the voltage showed two upticks, and eventually the NI coil experienced a thermal run-away from the point of passing 100 A, which was ~50 A above the I_C. A small hot spot occurred at Point A (>30 A above the I_C), but it was recovered by the self-protection and the excellent cooling capacity of liquid nitrogen. The partial small hot spot and recovery occurred again at Point B. In the case of the MI coil, the voltage increased quite slowly up to ~86 A, and then gradually increased faster. At around 92 A (13 A above its I_C), the voltage rose rapidly, recovered for a while, but rose sharply again, leading to a thermal runaway. The testing was stopped to protect the MI coil to be used for the SSMI. The first quench point above the I_C of the MI coil, ΔI=13 A, was lower than that of the NI coil, ΔI=30 A, and the NI coil was eventually quenched at the current point above I_C, ΔI=50 A, whereas the MI coil was not recovered and seemed to quench, indicating a poorer self-protecting capability.

On the other hand, the voltage of the SSMI coil increased very slowly up to 125 A, which is about 44 A higher than its IC, and it was more stable than the NI coil. The SSMI did not experience any thermal runaway, indicating that it generates less turn-to-turn heating during over-current operation than the NI and the MI coils in the same liquid nitrogen cooling condition. At around 80 A (Point C in Fig. 4), significant differences were observed in the magnetic field plots between the MI and the SSMI coils. The magnetic field of the SSMI coil began to saturate, indicating that some currents were bypassing through the surface shunt (solder). This result further demonstrated the superior self-protecting capability of the SSMI winding method, which is based on its low turn-to-turn resistance due to the surface shunting. Additionally, it highlights the importance of considering the critical current calculation when using the 1 μV/cm criteria.

IV. Conclusion

This paper introduced the SSMI winding method, a promising SS-tape-co-winding NI or MI variant. The SSMI method retains the mechanical advantage of MI, allowing for lower overall current density without sacrificing operating current over I_C, while increasing the equivalent strength within the winding pack. Additionally, this method enhances the self-protecting capability of the coil, surpassing that of the NI coil. Through over-current and discharging tests on three coils (NI, MI, and SSMI), we have demonstrated that the SSMI coil is thermally stable even in the over-critical-current region due to its reduced characteristic resistance, which is the lowest among the three coils. Furthermore, by shunting the already-wound coil surface with solder or other conductive materials, the self-protecting capability can be reinforced and controlled flexibly after manufacturing and preliminary testing of the magnet coils. Future studies will explore the extra-shunted NI/MI winding method by settling on a reliable process and testing with different types of metals/solders to design and control the characteristic resistance.

References

[1] S. Hahn, D. K. Park, J. Bascuñán, and Y. Iwasa, "HTS pancake coils without turn-to-turn insulation," *IEEE Trans. Appl. Supercond.*, vol. 21, no. 3, pp. 1592–1595, Jun. 2011.

[2] X. Wang *et al.*, "Turn-to-turn contact characteristics for an equivalent circuit model of no-insulation ReBCO pancake coil," *Supercond. Sci. Technol.*, vol. 26, no. 3, Jan. 2013, Art. no. 035012.

[3] Y. Wang, W. K. Chan, and J. Schwartz, "Self-protection mechanisms in no-insulation (RE)$Ba_2Cu_3O_x$ high temperature superconductor pancake coils," *Supercond. Sci. Technol.*, vol. 29, no. 4, Mar. 2016, Art. no. 045007.

[4] R. Gyuráki, T. Benkel, F. Schreiner, F. Sirois, and F. Grilli, "Fluorescent thermal imaging of a non-insulated pancake coil wound from high temperature superconductor tape," *Supercond. Sci. Technol.*, vol. 32, no. 10, Aug. 2019, Atr. no. 105006.

[5] Y. Iwasa, *Case Studies in Superconducting Magnet*, 2nd ed. New York, NY, USA: Springer-Verlag, 2009.

[6] S. Hahn, D. K. Park, J. Voccio, J. Bascuñán, and Y. Iwasa, "No-Insulation (NI) HTS Inserts for >1 GHz LTS/HTS NMR Magnets," *IEEE Trans. Appl. Supercond.*, vol. 22, no. 3, Jun. 2012, Art. ID. 4302405.

[7] A. Molodyk *et al.*, "Development and large volume production of extremely high current density YBa2Cu3O7 superconducting wires for fusion," *Sci. Rep.*, vol. 11, no. 1, Jan. 2021, Art. no. 2084.

[8] M. Paidpilli and V. Selvamanickam, "Development of RE-Ba-Cu-O superconductors in the U.S. for ultra-high field magnets," *Supercond. Sci. Technol.*, vol. 35, no. 4, Feb. 2022, Art. no. 043001.

[9] H. Song, P. Brownsey, Z. Yifei, J. Waterman, T. Fukushima, and D. Hazelton, "2G HTS Coil Technology Development at SuperPower," *IEEE Trans. Appl. Supercond.*, vol. 23, no. 3, Jun. 2013, Art. no.4600806.

[10] T. Lecrevisse and Y. Iwasa, "A (RE)BCO Pancake Winding with Metal-as-Insulation," *IEEE Trans. Appl. Supercond.*, vol. 26, no. 3, Apr. 2016, Art. no. 4700405.

[11] T. Lécrevisse, A. Badel, T. Benkel, X. Chaud, P. Fazilleau, and P. Tixador, "Metal-as-insulation variant of no-insulation HTS winding technique: pancake tests under high background magnetic field and high current at 4.2 K," *Supercond. Sci. Technol.*, vol. 31, no. 5, Apr. 2018, Art. no. 055008.

[12] S. Noguchi et al., "Numerical investigation of metal insulation technique on turn-to-turn contact resistance of REBCO pancake coils," IEEE Trans. Appl. Supercond., vol. 27, no. 4, Jun. 2017, Art. no. 7700505.

[13] M. H. Sohn, K. Sim, B. Eom, H. S. Ha, H. Y. Kim, and K. Seong, "Controllability of the contact resistance of 2G HTS coil with metal insulation," IEEE Trans. Appl. Supercond., vol. 28, no. 3, Apr. 2018, Art. no. 4602705

[14] D. Park, W. Lee, J. Bascuñán, H. M. Kim, and Y. Iwasa, "A Cryogen-Free 25-T REBCO Magnet With the Extreme-No-Insulation Winding Technique," *IEEE Trans. Appl. Supercond.*, vol. 32, no. 6, pp. 1–5, Sep. 2022, Art no. 4602305.

[15] W. Lee, D. Park, J. Bascuñán, and Y. Iwasa, "Construction and test result of an all-REBCO conduction-cooled 23.5 T magnet prototype towards a benchtop 1 GHz NMR spectroscopy," *Supercond. Sci. Technol.*, vol. 35, no. 10, Aug. 2022, Art. no. 105007.

[16] F. Dong *et al.*, "On fault-mode phenomenon in no-insulation superconducting magnets: A preventive approach," *Appl. Phys. Lett.*, vol. 121, no. 19, Nov. 2022, Art. no. 194101.

[17] D. Park, J. Bascunan, P. C. Michael, J. Lee, S. Hahn, and Y. Iwasa, "Construction and Test Results of Coils 2 and 3 of a 3-Nested-Coil 800-MHz REBCO Insert for the MIT 1.3-GHz LTS/HTS NMR Magnet," *IEEE Trans. Appl. Supercond.*, vol. 28, no. 3, pp. 1–5, Apr. 2017, Art no. 4300205.

[18] J. Mun, C. Lee, K. Sim, C. Lee, M. Park, and S. Kim, "Electrical Characteristics of Soldered Metal Insulation REBCO Coil," *IEEE Trans. Appl. Supercond.*, vol. 30, no. 4, pp. 1–4, Jun. 2020, Art no. 4701904.

[19] J. Lee, J. Mun, J. Kim, and S. Kim, "Investigation on the Electrical Contact Resistance of Soldered Metal Insulation REBCO Coil," *IEEE Trans. Appl. Supercond.*, vol. 31, no. 5, pp. 1–5, Aug. 2021, Art no. 4601205.

[20] J. Lee, J. Mun, J. Kim, K. Sim, S. Hahn, and S. Kim, "A Study on the Electrical Contact Resistance and Thermal Conductivity of Soldered-Metal Insulation Coil With Conduction Cooling," *IEEE Trans. Appl. Supercond.*, vol. 32, no. 6, pp. 1–5, Sep. 2022, Art no. 4604805.

[21] Tsui, R. Mahmoud, E. Surrey, and D. Hampshire, "Superconducting and Mechanical Properties of Low-Temperature Solders for Joints," *IEEE Trans. Appl. Supercond.*, vol. 26, no. 3, pp. 1–4, Apr. 2016, Art no. 6900204.

[22] J. B. Song and S. Y. Hahn, "'Leak Current' correction for critical current measurement of no-insulation HTS coil," Progr. Supercond. Cryogenics, vol. 19, no. 2, pp. 48–52, 2017.